

Supporting Information for

**Carboxyl-functionalized ionic liquids enable green preparation of
chitosan-based ionic gel membranes for H₂S separation**

Ping Zhang^a, Hao Zhu^a, Zhuoheng Tu^{a,}, Xingbang Hu^a, Youting Wu^{a,*}*

^a Separation Engineering Research Center, Key Laboratory of Mesoscopic Chemistry
of MOE, School of Chemistry and Chemical Engineering, Nanjing University, Nanjing
210023, P. R. China

*Correspondence and requests for materials should be addressed to zhtu@nju.edu.cn;
ytwu@nju.edu.cn

Index

Gas permeability measurement

Fig. S1. Illustration of single gas permeation unit.

Fig. S2. Illustration of mixed gas permeation device.

Supplementary data

Fig. S3. ^1H (a) and ^{13}C NMR (b) spectra of [Cmmim]Br in D_2O .

Fig. S4. ^1H (a) and ^{13}C NMR (b) spectra of [Cmmim][Tf₂N] in DMSO-d6.

Fig. S5. TG and DTG curves of CS powder (a) and DTG curves of CFILs (b).

Table S1 Thermal stability and basic mechanical strength of the CFILs, CS/AA membrane and CS/CFIL gel membranes.

Table S2. The density and *FFV* of the CFILs, CS/AA membrane and CS/CFIL membranes.

Fig S6. The surface and cross-sectional SEM images of CS/AA membrane and CS/CFIL gel membranes.

Fig S7. Permeability of CH₄ (a), CO₂ (b) and H₂S (c) as a function of transmembrane pressure difference.

Table S3 Detailed single gas permeability and ideal permselectivity in CS/CFIL gel membranes at 40 °C.

Fig. S8. FT-IR spectra (a) and TG curves (b) of CS/Tf₂N gel membranes with different content of [Cmmim][Tf₂N].

Table S4 Solubility and diffusion data in CS/Tf₂N (1:2), CS/Tf₂N (1:3) and CS/Tf₂N/Cl gel membranes.

Fig. S9. The optimized structures of [Cmmim]Cl, (b, c) the optimized structures and the $\text{sign}(\lambda_2)\rho$ colored δg^{inter} isosurface (isovalue=0.0110) maps of [Cmmim]Cl–H₂S complexes (Bond distances (Angstrom, Å) and $\delta g^{\text{inter}}(\text{BCP})$ (a.u.) values are labelled. Color legend: N blue, C cyan, O red, H white, Cl green and S yellow).

Fig. S10. The optimized structures of [Cmmim]Br, (b, c) the optimized structures and the $\text{sign}(\lambda_2)\rho$ colored δg^{inter} isosurface (isovalue=0.0135) maps of [Cmmim]Br–H₂S complexes (Bond distances (Angstrom, Å) and $\delta g^{\text{inter}}(\text{BCP})$ (a.u.) values are labelled. Color legend: N blue, C cyan, O red, H white, Br reddish brown and S yellow).

Fig. S11. FT-IR spectra (a), ¹H NMR spectra (b) and ¹³C NMR spectra (c) of fresh (purple), H₂S-dissolved (brownish) and regenerated (green) [Cmmim][Tf₂N]. Regeneration condition: N₂ sweeping at 40 °C and 100 ml min⁻¹ flow rate for 2 h.

Table S5 H₂S/CO₂/CH₄ (20/20/60 mol%) mixed gas separation performance of CS/Tf₂N/Cl (1:1.6:0.4) gel membranes at 10.0 bar and different temperatures (40 °C or 60 °C).

Table S6 Comparison of H₂S separation performance of CS/CFIL gel membranes with those of other membranes in the literature.

Gas permeability measurement

The gas (H_2S , CO_2 and CH_4) permeation was determined by a custom-made, corrosion-resistant dual-chamber device using a variable-pressure constant-volume method. As depicted in [Fig. S1](#),¹⁻² to ensure a constant temperature during permeation testing, the permeation cell and gas cylinders were placed in a constant temperature oven with an accuracy of ± 0.1 °C. By using two absolute pressure transducers (Wideplus Precision Instruments Co., Ltd., with a precision of 0.001 bar), the pressures of the upper (feed side) and lower (permeate side) chambers were collected and were recorded by a computer-aided data acquisition system. In a specific test, the CS gel membrane was first secured to a homemade stainless-steel tray with a loop of adhesive and then placed into the measurement device. The permeation unit was pumped to vacuum with an oil pump, and then 1.0 bar nitrogen (N_2) was introduced as an equilibrium gas, and it was considered to have been equilibrated when the pressure in the upper and lower chambers remained unchanged for at least 2 h. Subsequently, cut off the connection between two chambers, then a certain volume of the gas to be measured was introduced into the feed side and permeating across the membrane.

The gas permeation coefficient in the membrane was calculated using [Eq. \(S1\)](#) and [Eq. \(S2\)](#)

$$P = \frac{L}{\Delta p} \frac{V}{ART} \frac{dp_2}{dt} \quad (\text{S1})$$

$$\Delta p = p_1 - p_2 \quad (\text{S2})$$

where P represents the permeability coefficient (Barrer, 1 Barrer = 10^{-10} cm³ (STP)·cm·cm⁻²·s⁻¹·cmHg⁻¹), L stands for the thickness of the membrane (cm), V refers to the volume (cm³) of the lower chamber (permeate side) of the permeation cell, A is the effective area of the membrane (cm²), R is the ideal gas constant, T is the operating temperature (K), p_1 and p_2 are the pressures in the upper and lower chambers, respectively, and $\frac{dp_2}{dt}$ stands for the rate of the pressure increasing with time on the permeate side.

The ideal selectivity of gas pairs (S_{ij}) is calculated using [Eq. \(S3\)](#)

$$S_{i/j} = \frac{P_i}{P_j} \quad (\text{S3})$$

where P_i and P_j represent the permeation coefficients of gas i and j . After each experiment, the apparatus was evacuated and washed with N₂ at least five times.

The diffusion coefficient (D) was estimated from the time-lag method, using the following equation:

$$D = \frac{L^2}{6\theta} \quad (\text{S4})$$

where θ is lag time. The solubility coefficient (S) was calculated through the solution-diffusion model using [Eq. \(S5\)](#)

$$S = \frac{P}{D} \quad (\text{S5})$$

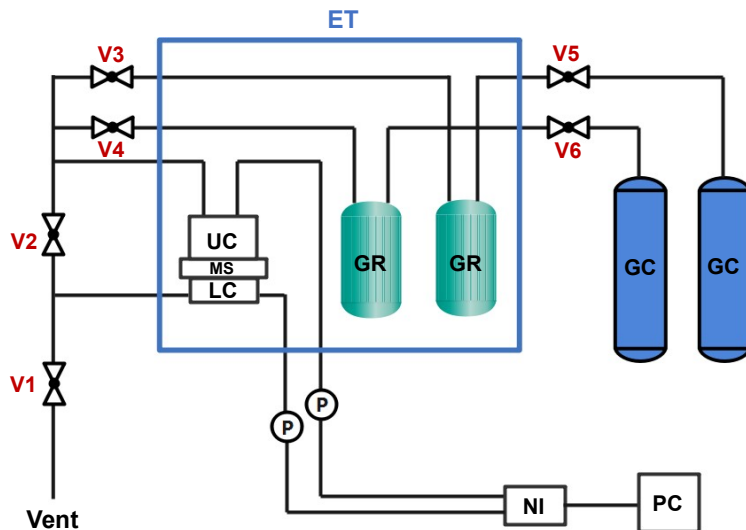


Fig. S1. Illustration of single gas permeation unit. (UC, upper chamber; LC, lower chamber; MS, membrane support; ET, electro-thermostatic oven; V1, V2, V3, V4, V5, V6, valves; GR, gas reservoir; GC, gas cylinder; P, pressure transducer; NI, numerical instrument; PC, personal computer).

A home-built Wicke-Kallenbach gas permeation setup was utilized to test the separation performance of H₂S/CO₂/CH₄ (20/20/60 mol%) mixed gas.³⁻⁴ As shown in **Fig. S2**, the permeation device was placed in an electro-thermostatic oven with a temperature accuracy of ± 0.1 °C to control the operating temperature. By using a backpressure valve (V2), the pressure on the feed side was controlled at 10.0 bar, and the permeate side pressure was set at 1.0 bar. Two absolute pressure sensors (Wideplus Precision Instruments Co., Ltd.) with an accuracy of 0.001 bar were used to accurately collect the pressure values on the feed side and permeate side chambers. The flow rates of the feed and sweep gas were controlled at 100 and 100 standard cubic centimeter per minute (sccm), respectively, using two mass flow controllers (DT-MFC/D, Nanjing Detu Technology Co., Ltd., China). A mass flowmeter (DT-MFM/D, Nanjing Detu

Technology Co., Ltd., China) was exploited to record flow rate on the permeate side. Leveraging gas analyzers (FORTUNE FZ800, Fucaiysi Scientific Instrument Co., LTD., China) with an accuracy of 1 ppm to determine the composition of the permeate gas stream. Gas permeability coefficients of H₂S, CO₂ and CH₄ were calculated using the following equation:

$$P_i = \frac{x_i \times S \times l}{A \times \Delta P_i} \quad (\text{S6})$$

where P_i is the permeability coefficient of gas i , x_i is the concentration of gas i in the permeate stream, S stands for the flow rate on the permeate side, l and A are membrane thickness and effective area, respectively, ΔP_i is the transmembrane partial pressure difference of gas i .

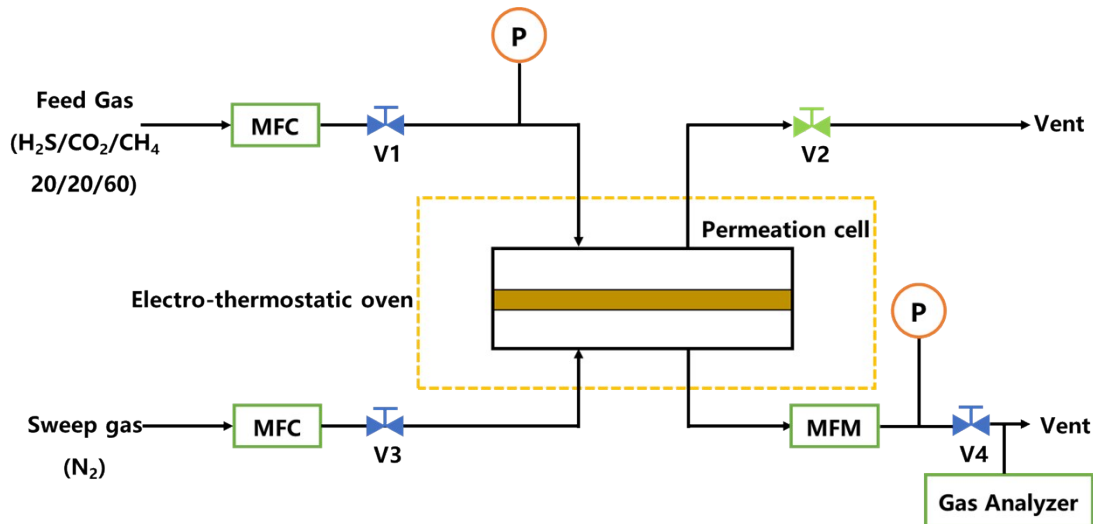


Fig. S2. Illustration of mixed gas permeation device. (MFC, mass flow controllers; MFM, mass flowmeter; P, pressure transducers; V2, backpressure valve; V1, V3, V4: needle valves)

Supplementary data

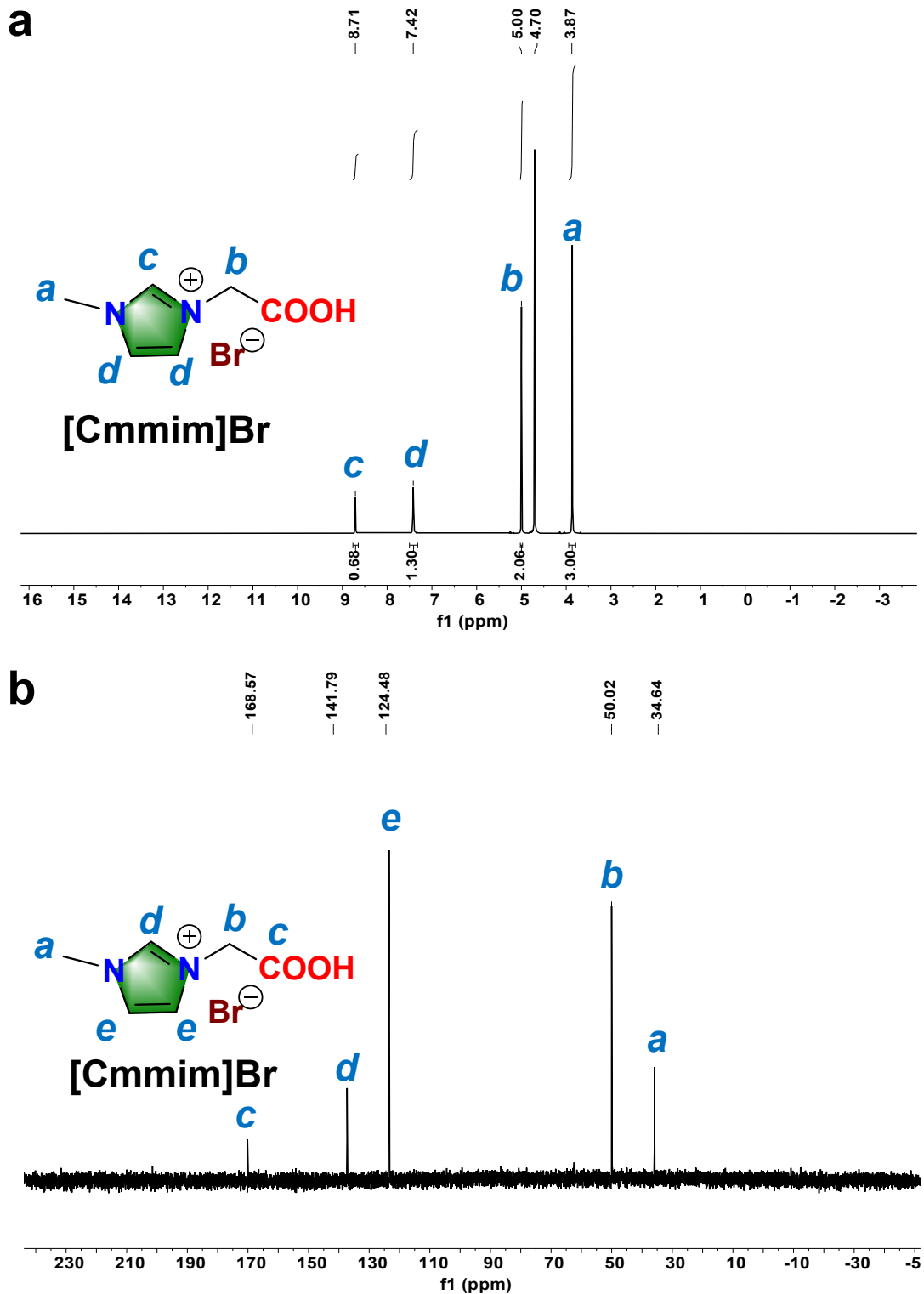


Fig. S3. ^1H (a) and ^{13}C NMR (b) spectra of $[\text{Cmmim}]\text{Br}$ in D_2O .

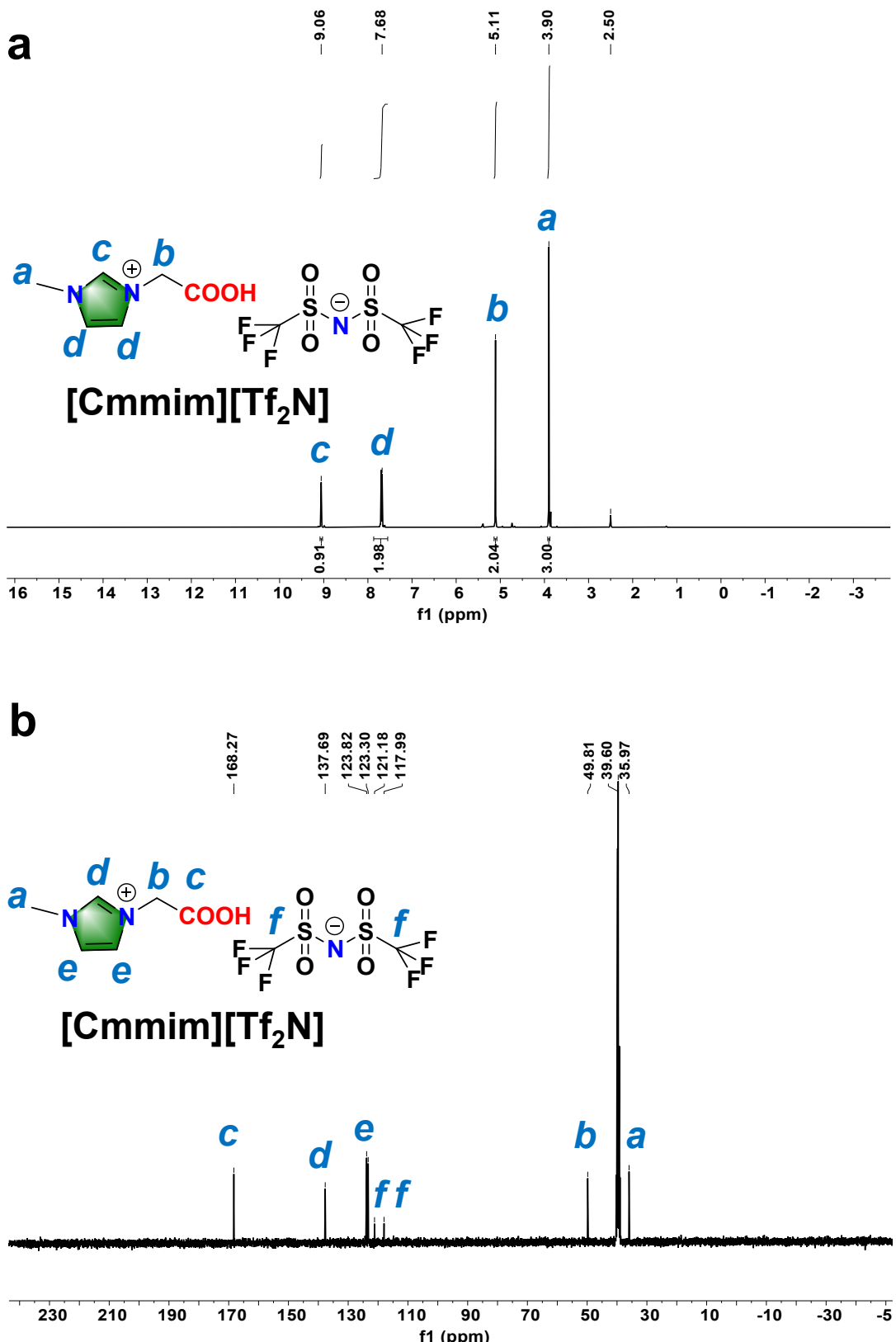


Fig. S4. ^1H (a) and ^{13}C NMR (b) spectra of $[\text{Cmmim}][\text{Tf}_2\text{N}]$ in DMSO-d_6 .

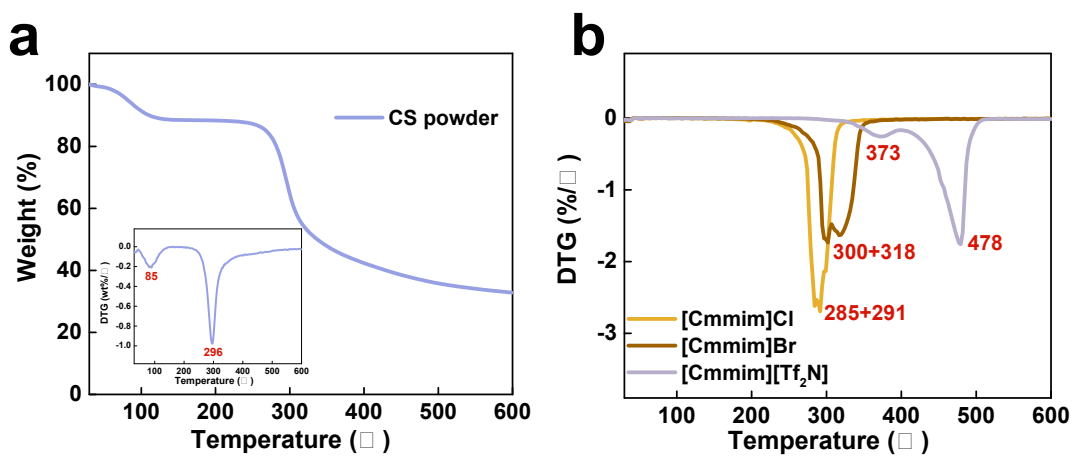


Fig. S5. TG and DTG curves of CS powder (a) and DTG curves of CFILs (b).

Table S1 Thermal stability and basic mechanical strength of the CFILs, CS/AA membrane and CS/CFIL gel membranes.

Samples	T _d (°C)	Tensile strength (MPa)	Yang's modulus (MPa)	Elongation at break (%)
CS/AA (1:1)	102	19.3	217	23.4
CS/Cl (1:1)	202	24.6	234	18.7
CS/Br (1:1)	202	24.5	231	17.8
CS/Tf₂N (1:1)	219	16.3	96.7	37.6
CS/Tf₂N (1:2)	257	5.02	18.1	50.2
CS/Tf₂N (1:4)	287	1.51	3.54	76.1
CS/Tf₂N (1:6)	317	0.975	1.31	76.6
CS/Tf₂N/Cl (1:1.8:0.2)	222	6.77	22.3	28.6
CS/Tf₂N/Cl (1:1.6:0.4)	219	7.40	38.2	24.5
CS/Tf₂N/Cl (1:2.7:0.3)	227	2.52	26.8	28.6
[Cmmim]Cl	254	-	-	-
[Cmmim]Br	267	-	-	-
[Cmmim][Tf₂N]	357	-	-	-

Table S2. The density and *FFV* of the CFILs, CS/AA membrane and CS/CFIL membranes.

Samples	Density (g/cm³)	FFV (%)
CS/AA (1:1)	1.473	8.54
CS/Cl (1:1)	1.507	6.17
CS/Br (1:1)	1.483	6.13
CS/Tf₂N (1:1)	1.545	18.6
[Cmmim]Cl	1.308	-
[Cmmim]Br	1.325	-
[Cmmim][Tf₂N]	1.778	-

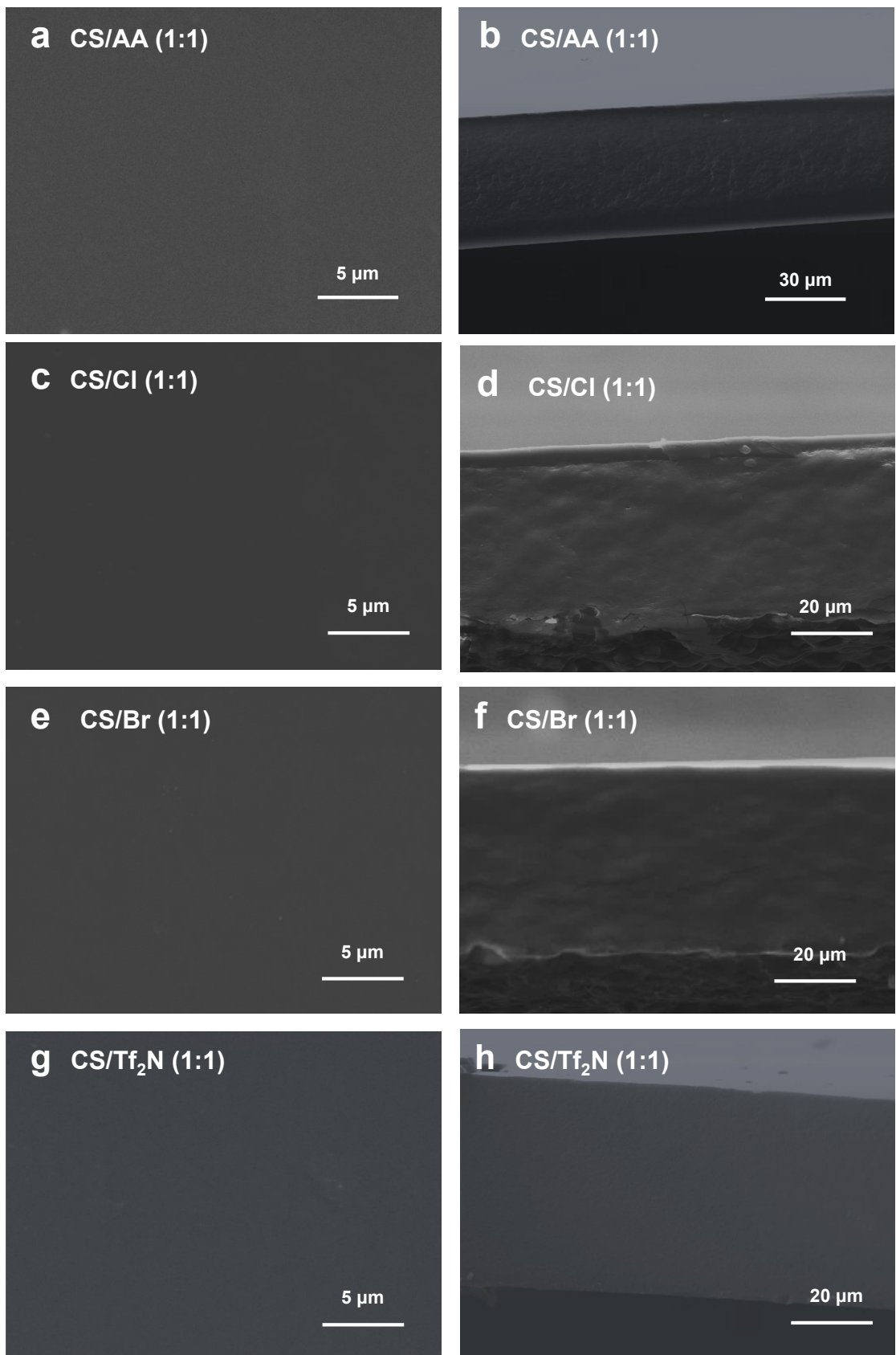


Fig S6. The surface and cross-sectional SEM images of the CS/AA membrane and CS/CFIL gel membranes.

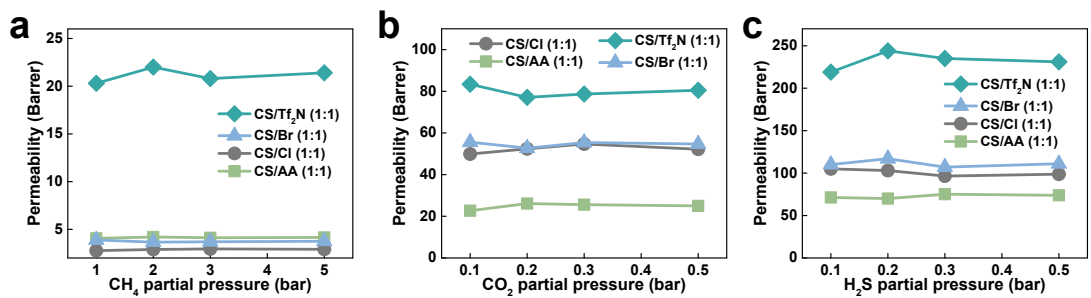


Fig S7. Permeability of CH₄ (a), CO₂ (b) and H₂S (c) as a function of transmembrane pressure difference.

Table S3 Detailed single gas permeability and ideal permselectivity in CS/CFIL gel membranes at 40 °C.

H₂S		CO₂		CH₄		Selectivity		
<i>p</i> (bar)	<i>P_{H2S}</i> (Barrer)	<i>p</i> (bar)	<i>P_{CO2}</i> (Barrer)	<i>p</i> (bar)	<i>P_{CH4}</i> (Barrer)	<i>S_{H2S/CH4}</i>	<i>S_{CO2/CH4}</i>	<i>S_{(H2S+CO2)/CH4}</i>
CS/AA (1:1)								
0.10	71.3	0.10	22.7	1.0	4.06	17.6	5.59	23.2
0.20	70.0	0.20	26.1	2.0	4.20	16.7	6.21	22.9
0.30	75.1	0.30	25.6	3.0	4.12	18.2	6.21	24.4
0.50	73.8	0.50	25.0	5.0	4.15	17.8	6.02	23.8
CS/Cl (1:1)								
0.10	105	0.10	49.9	1.0	2.77	37.9	18.0	55.9
0.20	103	0.20	52.4	2.0	2.89	35.6	18.1	53.8
0.30	96.5	0.30	54.7	3.0	2.95	32.7	18.5	51.3
0.50	98.7	0.50	52.2	5.0	2.91	33.9	17.9	51.9
CS/Br (1:1)								
0.10	110	0.10	55.6	1.0	3.89	28.3	14.3	42.6
0.20	117	0.20	52.7	2.0	3.66	32.0	14.4	46.4
0.30	107	0.30	55.4	3.0	3.70	28.9	15.0	43.9
0.50	111	0.50	54.7	5.0	3.75	29.6	14.6	44.2
CS/Tf₂N (1:1)								
0.10	219	0.10	83.4	1.0	20.3	10.8	4.11	14.9
0.20	244	0.20	77.1	2.0	22.0	11.1	3.50	14.6
0.30	235	0.30	78.7	3.0	20.8	11.3	3.78	15.1
0.50	231	0.50	80.5	5.0	21.4	10.8	3.76	14.6
CS/Tf₂N (1:2)								
0.50	412	0.50	139	5.0	39.6	10.4	3.50	13.9
CS/Tf₂N (1:3)								
0.50	593	0.50	190	5.0	58.8	10.1	3.22	13.32
CS/Tf₂N (1:4)								

0.50	843	0.50	257	5.0	84.3	10.0	3.05	13.1
CS/Tf₂N (1:6)								
0.50	890	0.50	275	5.0	90.0	9.89	3.06	13.0
CS/Tf₂N/Cl (1:1.8:0.2)								
0.50	505	0.50	195	5.0	25.4	19.9	7.69	27.6
CS/Tf₂N/Cl (1:1.6:0.4)								
0.50	642	0.50	287	5.0	22.1	29.1	13.0	42.1
CS/Tf₂N/Cl (1:2.7:0.3)								
0.50	696	0.50	327	5.0	39.1	17.8	8.4	26.2
CS/Tf₂N/Cl (1:1.6:0.4) recycled 1								
0.50	613	0.50	266	5.0	21.4	28.6	12.4	41.1
CS/Tf₂N/Cl (1:1.6:0.4) recycled 2								
0.50	594	0.50	251	5.0	20.9	28.4	12.0	40.4
CS/Tf₂N/Cl (1:1.6:0.4) recycled 3								
0.50	585	0.50	253	5.0	21.2	27.6	11.9	39.5
CS/Tf₂N/Cl (1:1.6:0.4) recycled 4								
0.50	598	0.50	246	5.0	20.2	29.6	12.2	41.8
CS/Tf₂N/Cl (1:1.6:0.4) recycled 5								
0.50	590	0.50	243	5.0	20.5	28.8	11.9	40.6

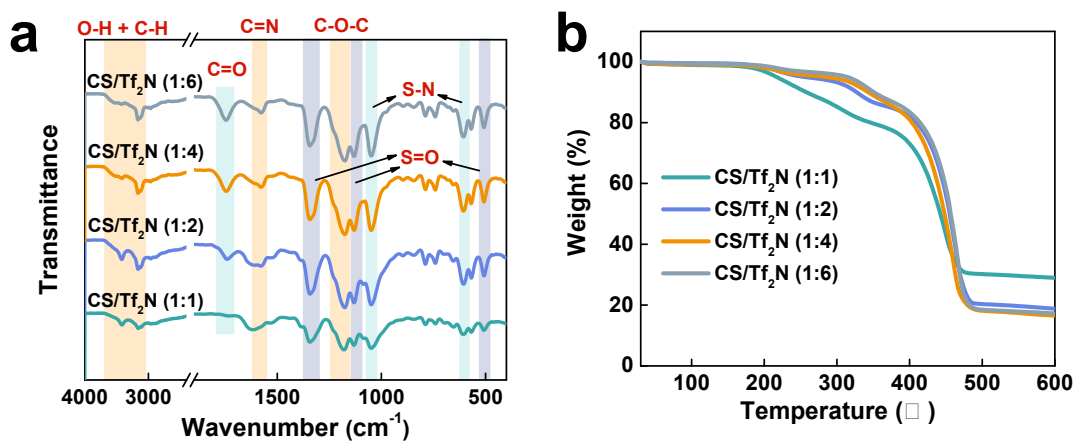


Fig. S8. FT-IR spectra (a) and TG curves (b) of CS/Tf₂N gel membranes with different content of [Cmmim][Tf₂N].

Table S4 Solubility and diffusion data in CS/Tf₂N (1:2), CS/Tf₂N (1:3) and CS/Tf₂N/Cl gel membranes.

Membranes	Solubility coefficient (10 ⁻¹ cm ³ (STP)/(cm ³ cmHg))			Solubility selectivity		Diffusion coefficient (10 ⁻⁹ cm ² /s)			Diffusion selectivity	
	H ₂ S	CO ₂	CH ₄	H ₂ S/CH ₄	CO ₂ /CH ₄	H ₂ S	CO ₂	CH ₄	H ₂ S/CH ₄	CO ₂ /CH ₄
CS/Tf ₂ N (1:2)	40.68	18.32	18.38	2.213	0.9964	10.13	7.573	2.154	4.704	3.516
CS/Tf ₂ N/Cl (1:1.8:0.2)	62.43	26.73	12.93	5.024	2.151	8.091	7.309	1.964	3.958	3.576
CS/Tf ₂ N/Cl (1:1.6:0.4)	85.12	39.89	12.12	7.678	3.598	7.541	7.196	1.819	3.791	3.618
CS/Tf ₂ N (1:3)	33.05	16.28	19.13	1.728	0.8511	18.55	11.65	3.075	6.032	3.789
CS/Tf ₂ N/Cl (1:2.7:0.3)	49.96	35.76	14.64	3.158	2.261	13.92	9.154	2.675	5.625	3.699

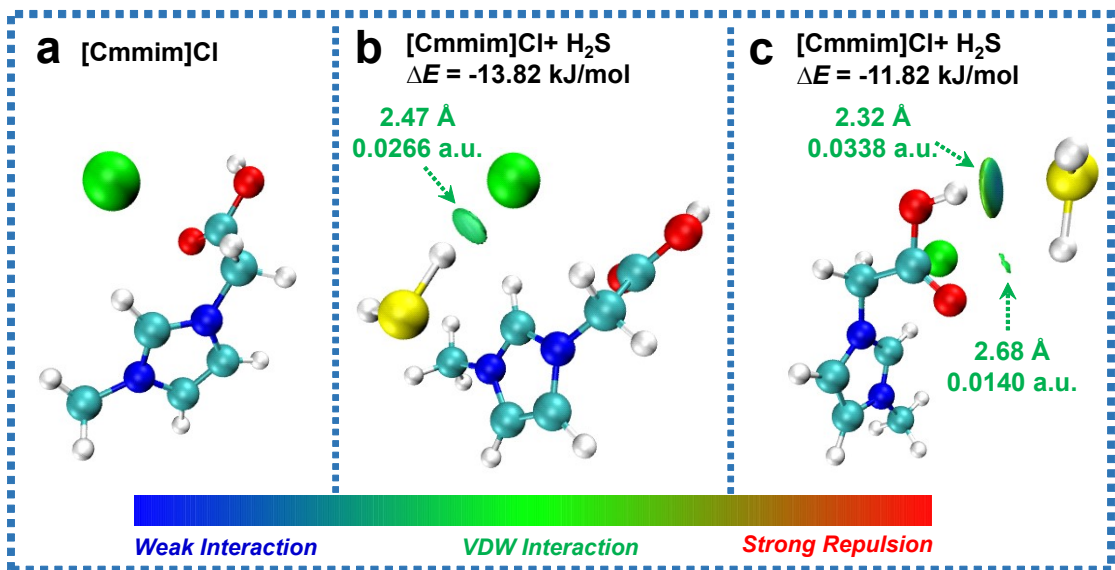


Fig. S9. The optimized structures of [Cmmim]Cl, (b, c) the optimized structures and the $\text{sign}(\lambda_2)\rho$ colored δg^{inter} isosurface (isovalue=0.0110) maps of [Cmmim]Cl–H₂S complexes (Bond distances (Angstrom, Å) and $\delta g^{\text{inter}}(\text{BCP})$ (a.u.) values are labelled. Color legend: N blue, C cyan, O red, H white, Cl green and S yellow).

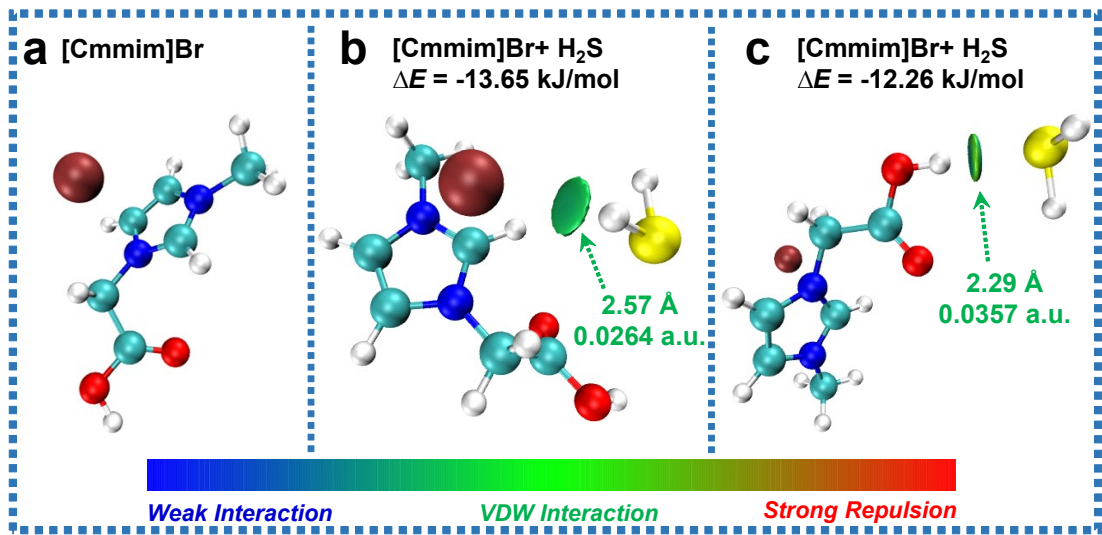


Fig. S10. The optimized structures of [Cmmim]Br, (b, c) the optimized structures and the $\text{sign}(\lambda_2)\rho$ colored δg^{inter} isosurface (isovalue=0.0135) maps of [Cmmim]Br–H₂S complexes (Bond distances (Angstrom, Å) and $\delta g^{\text{inter}}(\text{BCP})$ (a.u.) values are labelled. Color legend: N blue, C cyan, O red, H white, Br reddish brown and S yellow).

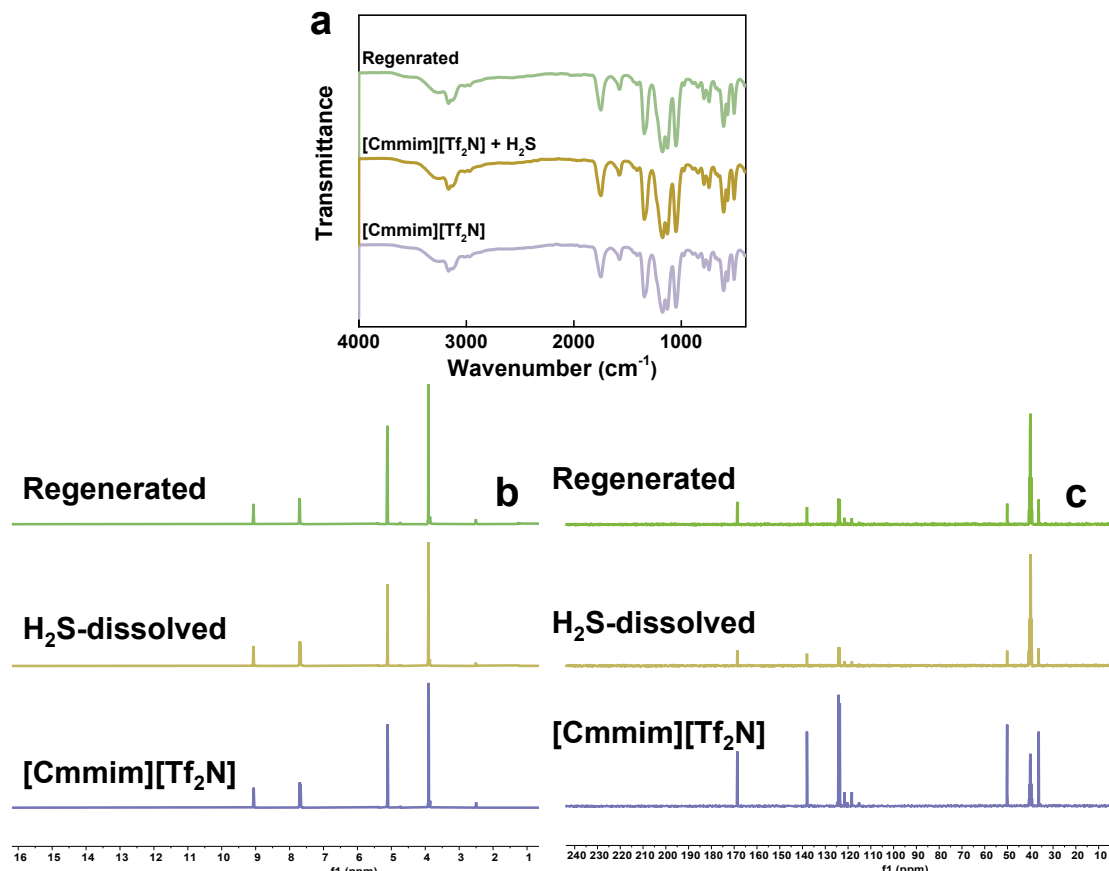


Fig. S11. FT-IR spectra (a), ^1H NMR spectra (b) and ^{13}C NMR spectra (c) of fresh (purple), H_2S -dissolved (brownish) and regenerated (green) $[\text{Cmmim}][\text{Tf}_2\text{N}]$. Regeneration condition: N_2 sweeping at 40°C and 100 ml min^{-1} flow rate for 2 h.

Table S5 H₂S/CO₂/CH₄ (20/20/60 mol%) mixed gas separation performance of CS/Tf₂N/Cl (1:1.6:0.4) gel membranes at 10.0 bar and different temperatures (40 °C or 60 °C).

<i>t</i> (h)	<i>P</i> _{H₂S} (Barrer)	<i>P</i> _{CO₂} (Barrer)	<i>P</i> _{CH₄} (Barrer)	<i>S</i> _{H₂S/CH₄}	<i>S</i> _{CO₂/CH₄}	<i>S</i> _{(H₂S+CO₂)/CH₄}
0	547	236	21.6	25.3	10.9	36.3
2	568	247	22.3	25.5	11.1	36.5
4	559	240	23.1	24.2	10.4	34.6
6	552	235	22.7	24.3	10.4	34.7
8	545	232	21.7	25.1	10.7	35.8
10	529	227	21.3	24.8	10.7	35.5
13	535	230	21.5	24.9	10.7	35.6
16	518	222	21.2	24.4	10.5	34.9
19	509	214	20.9	24.4	10.2	34.6
22	514	213	21.1	24.4	10.1	34.5
25	527	220	22.0	24.0	10.0	34.0
28	520	217	21.4	24.3	10.1	34.4
33	817	340	35.0	23.3	9.71	33.1
37	851	362	36.7	23.2	9.86	33.1
41	848	358	36.5	23.2	9.81	33.0
45	844	355	35.9	23.5	9.89	33.4
50	836	350	36.3	23.0	9.64	32.7
55	854	345	36.6	23.3	9.43	32.8
60	850	359	36.0	23.6	9.97	33.6
65	832	347	35.5	23.4	9.77	33.2
70	825	338	35.4	23.3	9.55	32.9
75	517	219	21.0	24.6	10.4	35.0
80	518	215	20.8	24.9	10.3	35.2
85	524	220	21.3	24.6	10.3	34.9
90	532	222	21.1	25.2	10.5	35.7
95	519	217	20.5	25.3	10.6	35.9
100	524	224	20.9	25.1	10.7	35.8

Table S6 Comparison of H₂S separation performance of CS/CFIL gel membranes with those of other membranes in the literature.

Membranes	Categories	Permeability (Barrer)			Selectivity (H ₂ S+CO ₂)/CH ₄	Ref.
		H ₂ S	CO ₂	CH ₄		
CS/AA (1:1) ^a	Polymer membrane	73.8	25.0	4.15	23.8	This work
CS/Cl (1:1) ^a	Gel membrane	98.7	52.2	2.91	51.9	This work
CS/Br (1:1) ^a	Gel membrane	111	54.7	3.75	44.1	This work
CS/Tf ₂ N (1:1) ^a	Gel membrane	231	80.5	21.4	14.6	This work
CS/Tf ₂ N (1:2) ^a	Gel membrane	412	139	39.6	13.9	This work
CS/Tf ₂ N (1:3) ^a	Gel membrane	613	190	58.8	13.7	This work
CS/Tf ₂ N (1:4) ^a	Gel membrane	842	257	84.3	13.1	This work
CS/Tf ₂ N (1:6) ^a	Gel membrane	890	275	90.0	13.0	This work
CS/Tf ₂ N/Cl (1:1.8:0.2) ^a	Gel membrane	505	195	25.4	27.6	This work
CS/Tf ₂ N/Cl (1:1.6:0.4) ^a	Gel membrane	642	287	22.1	42.1	This work
CS/Tf ₂ N/Cl (1:2.7:0.3) ^a	Gel membrane	696	327	39.2	26.1	This work
CS/Tf ₂ N/Cl (1:1.6:0.4) ^b	Gel membrane	535	228	21.7	35.1	This work
CS/Tf ₂ N/Cl (1:1.6:0.4) ^c	Gel membrane	840	350	36.0	33.1	This work
CS/Tf ₂ N/Cl (1:1.6:0.4) recycled 1 ^a	Gel membrane	613	266	21.4	41.1	This work
CS/Tf ₂ N/Cl (1:1.6:0.4) recycled 2 ^a	Gel membrane	594	251	20.9	40.4	This work
CS/Tf ₂ N/Cl (1:1.6:0.4) recycled 5 ^a	Gel membrane	590	243	20.5	40.6	This work
CA ^d	Polymer membrane	39.7	27.5	1.45	46.5	5
CA ^e	Polymer membrane	2.13	2.43	0.11	41	6
PU1 ^f	Polymer membrane	183	55.8	7.96	29.9	6
PU2 ^f	Polymer membrane	618	195	34.3	23.6	6
PU3 ^f	Polymer membrane	280	62.2	5.09	67	6
PU4 ^f	Polymer membrane	223	50.8	3.38	81	6
Pebax MX 1074 ^g	Polymer membrane	553	122	10.2	66	6
Pebax MX 1657 ^g	Polymer membrane	248	69.1	4.86	65	6

Pebax MX 1041^g	Polymer membrane	175	39.7	3.57	60	6
PIM-6FDA-OH^h	Polymer membrane	63	52.6	2.1	55	7
6FDA-DAM:DABA (3:2)ⁱ	Polymer membrane	106.7	97.7	4.36	46.92	8
6FDA-DAM^j	Polymer membrane	1076	737	27.9	65.2	9
6FDA-DAM/DABA 200 °C^j	Polymer membrane	87.4	91	1.78	99.7	9
6FDA-CARDO(<i>t</i>-Bu)^k	Polymer membrane	148	95.1	9.20	26.4	10
6FDA-DAM/CARDO (1:3)^l	Polymer membrane	70.9	56.0	3.04	41.8	11
PI-Br^m	Polymer membrane	144	92.0	5.28	44.7	12
Cross-linked DEGMCⁿ	Polymer membrane	55.2	38.2	2.86	47.7	13
Cross-linked TEGMC^o	Polymer membrane	40.5	50	1.72	52.5	13
PEG1000^p	Polymer membrane	25.9	5.2	0.23	132.5	14
TFC low P membrane^q	Polymer membrane	21	18.9	6.00	8.5	15
TFC high P membrane^q	Polymer membrane	62	52.1	3.54	32.3	15
Pebax 1657^r	Polymer membrane	383	102	6.30	77.0	16
Pebax/TFA-100^r	Blended membrane	2383	617	43.7	68.6	16
[Emim][EtSO₄]^s	Blended membrane	540	55.0	11.9	50	17
[Bmim][PF₆]^t	Supported membrane	1907	512	63.9	29.8	18
[Bmim][Tf₂N]^t	Supported membrane	2600	1233	131	29.2	18
[DMPDAH][Tf₂N]^u	Supported membrane	929	1270	38.1	24.4	19
[Bmim][BF₄]^v	Supported membrane	142	70	8.6	16.4	20
30.05 wt% Y-fum-fcu-MOF/6FDA-DAM^w	Mixed matrix membrane	469.8	587.9	20.1	52.8	21
19.0 wt% Eu-naph-fcu-MOF/6FDA-DAM^w	Mixed matrix membrane	287.4	460.4	15.2	49.2	21
17.7 wt% Y-fum-fcu-MOF/6FDA-DAM-DABA^w	Mixed matrix membrane	67.3	158.6	3.42	66.1	21
Zr-mfum-fcu-MOF/6FDA-DAM-20%^w	Mixed matrix membrane	218.8	320.1	9.81	54.7	22
Zr-mfum-fcu-MOF/6FDA-DAM-DABA-20%^w	Mixed matrix membrane	27.5	74.8	1.33	72.3	22

^a 0.50 bar of H₂S, 0.50 bar of CO₂, 5.0 bar of CH₄, 40 °C.

^b H₂S/CO₂/CH₄ (20/20/60 mol%) mixed gas, 10.0 bar, 40 °C.

^c H₂S/CO₂/CH₄ (20/20/60 mol%) mixed gas, 10.0 bar, 60 °C.

^d H₂S/CO₂/CH₄ (20/20/60%) mixed gas, 48.3 bar, 35 °C.

^e H₂S/CO₂/CH₄ (6/29/65%) mixed gas, 10 bar, 35 °C.

^f H₂S/CO₂/CH₄ (12.5/18.1/69.4%) mixed gas, 10 bar, 35 °C.

^g H₂S/CO₂/CH₄ (1.3/27.9/70.8%) mixed gas, 10 bar, 35 °C.

^h H₂S/CO₂/CH₄ (15/15/70%) mixed gas, 48.3 bar, 35 °C.

ⁱ H₂S/CO₂/CH₄ (25/5/70%) mixed gas, 48.3 bar, 35 °C.

^j H₂S/CO₂/CH₄ (0.5/20/79.5%) mixed gas, 6.9 bar, 35 °C.

^k H₂S/CO₂/CH₄/C₂H₆/N₂ (22/10/55/3/10%) mixed gas, 500 psi, 22 °C.

^l H₂S/CO₂/CH₄/C₂H₆/N₂ (20/10/57-59/3-1/10%) mixed gas, 34.5 bar, 22 °C.

^m H₂S/CO₂/CH₄/C₂H₆/N₂ (19.8/9.60/60.2/1/10.1%) mixed gas, 500 psi, 22 °C.

ⁿ H₂S/CO₂/CH₄ (20/20/60%) mixed gas, 55.2 bar, 35 °C.

^o H₂S/CO₂/CH₄ (20/20/60%) mixed gas, 48.3 bar, 35 °C.

^p H₂S/CO₂/CH₄ (5/3/92%) mixed gas, 56.7 bar, 25 °C.

^q H₂S/CO₂/CH₄ (0.1/46.6/53.3%) mixed gas, 5 bar.

^r 0.5 bar of H₂S, 0.15 bar of CO₂, 5.0 bar of CH₄, 40 °C.

^s 6.9 bar, 30 °C.

^t 0.1 bar, 40 °C.

^u 0.05 bar of H₂S and CO₂, 0.5 bar of CH₄, 40 °C.

^v H₂S/CO₂/CH₄ (5.3/18.2/76.5%) mixed gas, 2.0 bar, 25 °C.

^w H₂S/CO₂/CH₄ (20/20/60%) mixed gas, 6.9 bar, 35 °C.

References

- 1 P. Zhang, W. Xiong, M. Shi, Z. Tu, X. Hu, X. Zhang, Y. Wu, *Chem. Eng. J.*, 2022, **438**, 135626.
- 2 P. Zhang, Z. Tu, Z. Yan, X. Zhang, X. Hu, Y. Wu, *J. Hazard. Mater.*, 2023, **460**, 132515.
- 3 P. Zhang, Z. Tu, X. Hu, Y. Wu, *Sep. Purif. Technol.*, 2025, **359**, 130500.
- 4 Y. Cheng, X. Wang, C. Jia, Y. Wang, L. Zhai, Q. Wang, D. Zhao, *J. Membr. Sci.*, 2017, **539**, 213-223.
- 5 C.S.K. Achoundong, N. Bhuwania, S.K. Burgess, O. Karvan, J.R. Johnson, W.J. Koros, *Macromolecules*, 2013, **46**, 5584-5594.
- 6 A.A.H. G.Chatterjee, S.A. Stern, *J. Membr. Sci.*, 1997, **135**, 99-106.
- 7 S. Yi, X. Ma, I. Pinna, W.J. Koros, *J. Mater. Chem. A*, 2015, **3**, 22794-22806.
- 8 Z. Liu, Y. Liu, W. Qiu, W.J. Koros, *Angew. Chem. Int. Ed.*, 2020, **59**, 14877-14883.
- 9 Y. Liu, Z. Liu, G. Liu, W. Qiu, N. Bhuwania, D. Chinn, W.J. Koros, *J. Membr. Sci.*, 2020, **593**, 117430.
- 10 G.O. Yahaya, A. Hayek, A. Alsamah, Y.A. Shalabi, M.M. Ben Sultan, R.H. Alhajry, *Sep. Purif. Technol.*, 2021, **272**, 118897.
- 11 A. Hayek, A. Alsamah, G.O. Yahaya, E.A. Qasem, R.H. Alhajry, *J. Mater. Chem. A*, 2020, **8**, 23354-23367.
- 12 A. Hayek, A. Alsamah, Q. Saleem, R.H. Alhajry, A.A. Alsuwailem, *J. Membr. Sci.*, 2025, **721**, 123807.
- 13 Y. Liu, Z. Liu, B.E. Kraftschik, V.P. Babu, N. Bhuwania, D. Chinn, W.J. Koros, *J. Membr. Sci.*, 2021, **632**, 119361.
- 14 D.J. Harrigan, J.A. Lawrence, H.W. Reid, J.B. Rivers, J.T. O'Brien, S.A. Sharber, B.J. Sundell, *J. Membr. Sci.*, 2020, **602**, 117947.
- 15 P. Dolejš, V. Poštulka, Z. Sedláčková, V. Jandová, J. Vejražka, E. Esposito, J.C. Jansen, P. Izák, *Sep. Purif. Technol.*, 2014, **131**, 108-116.
- 16 P. Zhang, X. Ma, Z. Tu, X. Zhang, X. Hu, Y. Wu, *Green Energy Environ.*, 2025, **10**, 560-572.
- 17 M. Bhattacharya, M.K. Mandal, *J. Clean. Prod.*, 2017, **156**, 174-183.
- 18 X. Zhang, Z. Tu, H. Li, K. Huang, X. Hu, Y. Wu, D.R. MacFarlane, *J. Membr. Sci.*, 2017, **543**, 282-287.
- 19 L. Peng, M. Shi, X. Zhang, W. Xiong, X. Hu, Z. Tu, Y. Wu, *Green Chem. Eng.*, 2022, **3**, 259-266.
- 20 A. Akhmetshina, N. Yanbikov, A. Atlaskin, M. Trubyanov, A. Mechergui, K. Otvagina, E. Razov, A. Mochalova, I. Vorotyntsev, *Membranes*, 2019, **9**, 9.
- 21 G. Liu, V. Chernikova, Y. Liu, K. Zhang, Y. Belmabkhout, O. Shekhah, C. Zhang, S. Yi, M. Eddaoudi, W.J. Koros, *Nat. Mater.*, 2018, **17**, 283-289.
- 22 Y. Liu, Z. Chen, W. Qiu, G. Liu, M. Eddaoudi, W.J. Koros, *J. Membr. Sci.*, 2021, **627**, 119201.